

# Optical Control of Photogenerated Ion Pair Lifetimes: An Approach to a Molecular Switch

Martin P. Debreczeny, Walter A. Svec, Michael R. Wasielewski\*

A prototype molecular switch is demonstrated that works on the principle that the local electric field produced by one photogenerated ion pair ( $D_1^+ - A_1^-$ ) can influence the rate constants for photoinduced electron transfer and recombination in a second donor-acceptor pair ( $A_2 - D_2$ ). Two ultrafast laser pulses were used to control the rate of a photoinduced electron transfer reaction within a molecule that consists of two covalently linked electron donor-acceptor pairs fixed in a linear structure,  $D_1 - A_1 - A_2 - D_2$ . This type of molecular architecture may lead to the development of electronic devices that function on the molecular length scale.

Donor-acceptor arrays that undergo photoinduced electron transfer reactions are promising as molecular electronic devices because many of these reactions are reversible, occur with high quantum efficiency, and proceed with subpicosecond time constants (1–6). One method of controlling the rates of electron transfer reactions is through the application of electric fields. As a consequence, a considerable amount of work has been devoted to the theoretical modeling (7–9) and experimental realization (10–12) of molecular electronic switches consisting of organic electron donor-acceptor pairs whose function is controlled by an external electric field. Langmuir-Blodgett films containing monolayers of donor and acceptor chromophores have been created in which control of electron transfer was achieved by varying the layer composition separating the donors and acceptors and by the application of external fields (13, 14).

Recently, it was shown that the electric dipole of a synthetic  $\alpha$ -helical polypeptide can influence the rate of electron transfer between organic electron donors and acceptors covalently attached to the polypeptide (15). The electric field produced by a photogenerated ion pair can, in turn, have a large effect on the electronic states of surrounding molecules. We have studied covalently linked donor-acceptor-probe molecular arrays that undergo photoinduced charge separation in  $<10$  ps in low-polarity solvents (16, 17). These photogenerated donor<sup>+</sup>-acceptor<sup>-</sup> ion pairs produce an electric field of  $6 \text{ MV cm}^{-1}$ , which shifts the optical absorption spectra of the probe molecules by 5 to 15 nm.

These results suggest that it might be

possible to use the large, anisotropic, local electric fields generated by the formation of ion pairs to control a second photoinduced electron transfer reaction on a picosecond time scale. The use of photogenerated ion pairs to generate an electric field at the molecular level holds several advantages over external, macroscopic field generation: (i) the applied field strength can be larger, that is, macroscopic field strengths are limited by dielectric breakdown; (ii) the field can be turned on and off on a picosecond time scale; (iii) the electric field is under optical control; and (iv) only a very small volume is affected by the locally applied electric field. Here, we describe a donor<sub>1</sub>-acceptor<sub>1</sub>-acceptor<sub>2</sub>-donor<sub>2</sub> molecule ( $D_1 - A_1 - A_2 - D_2$ , Fig. 1) (18) in which photoinduced charge separation within one donor-acceptor pair controls the rate constants for photoinduced charge separation and thermal charge recombination within a second donor-acceptor pair. Multiple 150-fs laser pulses are used to selectively control and probe the generation of the two ion pairs (19).

For the electric field-induced switching

effect to be observed, the  $D_1 - A_1 - A_2 - D_2$  molecule must fulfill several major requirements. First, it must be possible to selectively excite the two donors,  $D_1$  and  $D_2$ . Zinc 5-phenyl-10,15,20-tri(*n*-pentyl)porphyrin ( $D_1$ ) and the phenyldimethylpyrromethene dye ( $D_2$ ) were chosen for this purpose because they can be independently excited at 416 and 512 nm, respectively. Second, the two acceptors,  $A_1$  and  $A_2$ , should be transparent at the two excitation wavelengths in either their neutral or singly reduced states. However, they should have strong absorptions at other wavelengths that are independently observable when  $A_1$  and  $A_2$  are reduced. 1,4:5,8-Naphthalenediimide ( $A_1$ ) and pyromellitimide ( $A_2$ ) were chosen because they absorb weakly at 416 and 512 nm in their ground states, and their radical anion spectra have well-separated absorptions at 480 and 713 nm, respectively (20, 21). Third, the population of field-generating ion pairs,  $D_1^+ - A_1^-$ , within  $D_1 - A_1 - A_2 - D_2$  must be large enough to affect the electron transfer reactions of  $A_2 - D_2$ . This was achieved by choosing a porphyrin with a large absorption cross section at the 416-nm excitation wavelength ( $\epsilon_{416} = 10^5 \text{ M}^{-1} \text{ cm}^{-1}$ ) as  $D_1$  (22, 23). Fourth, redox potentials for the one-electron oxidation of  $D_1$  and  $D_2$  as well as for the one-electron reduction of  $A_1$  and  $A_2$  must be chosen to ensure that charge separation and recombination occurs only within each individual donor-acceptor pair,  $D_1 - A_1$  and  $A_2 - D_2$ . Fifth, the free energies for photoinduced charge separation from the lowest excited singlet states of the donors within each pair to their corresponding acceptors should be sufficiently negative to ensure rapid rates of ion pair formation in the low-polarity solvents necessary to support large electric fields. The redox potentials for  $D_1$ ,  $A_1$ ,  $A_2$ ,

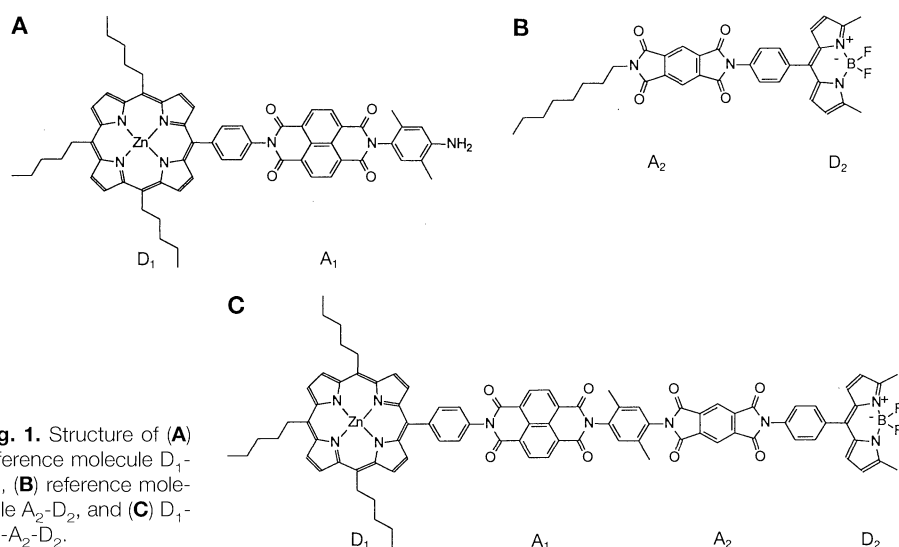


Fig. 1. Structure of (A) reference molecule  $D_1 - A_1$ , (B) reference molecule  $A_2 - D_2$ , and (C)  $D_1 - A_1 - A_2 - D_2$ .

M. P. Debreczeny and W. A. Svec, Chemistry Division, Argonne National Laboratory, Argonne, IL 60439, USA. M. R. Wasielewski, Chemistry Division, Argonne National Laboratory, Argonne, IL 60439, USA, and Department of Chemistry, Northwestern University, Evanston, IL 60208, USA.

\*To whom correspondence should be addressed.

and  $D_2$ , as well as the lowest excited singlet-state energies for  $D_1$  and  $D_2$ , fulfill the fourth and fifth requirements (24).

Single-pulse excitation of  $D_1-A_1-A_2-D_2$  in 1,4-dioxane at either 416 nm ( $^1D_1$ ) or 512 nm ( $^1D_2$ ) led to ion pair formation of either  $D_1^+-A_1^-$  or  $A_2^--D_2^+$ , respectively, as was monitored at 480 nm ( $A_1^-$ ) or 713 nm ( $A_2^-$ ) (Fig. 2). The time constants for ion pair formation and decay of either  $D_1^+-A_1^-$  or  $A_2^--D_2^+$  within  $D_1-A_1-A_2-D_2$  are similar to those observed for the  $D_1-A_1$  and  $A_2-D_2$  reference compounds (Fig. 1). In the two-pump pulse experiment, a single 512-nm pulse again produced  $D_1-A_1-A_2^--D_2^+$ . The transient absorption signal for  $A_2^-$  within  $D_1-A_1-A_2^--D_2^+$  reached a maximum at  $\sim 700$  ps after the arrival of the 512-nm pulse. At that time, a second 416-nm pulse was used to produce  $^1D_1-A_1-A_2^--D_2^+$ , which underwent rapid electron transfer from  $^1D_1$  to yield  $D_1^+-A_1^-A_2^--D_2^+$ . The solid curve in Fig. 2 does not directly reflect the kinetics of the  $D_1^+-A_1^-$  state because of the detection strategy (19) and because the probe at 713 nm monitors the population of  $A_2^-$  selectively. Instead, the effect of the electric field generated by the  $D_1^+-A_1^-$  state on the population of the  $A_2^--D_2^+$  state is observed (25).

An energetic and kinetic scheme was used to model the electric field effect (Fig. 3) (24). The basis for the model is simply that the rates of charge separation and recombination for each of the two donor-acceptor pairs will be different when the adjacent donor-acceptor pair is in a charge-separated state as opposed to the neutral state. These new electric field-modified rate constants for electron transfer and recombination are represented by primes in Fig. 3. In addition, the absorption cross sections for each species were varied to reflect the possibility that the electric field generated by one ion pair might shift the electronic absorptions of the ionic or neutral donor and acceptor within the other pair (26). The populations of all species were solved analytically and used to generate the fit shown (smooth solid line in Fig. 2). The observed kinetics are more sensitive to the electric field effect on the rate of recombination of the  $A_2^--D_2^+$  state to the ground state in the presence of the  $D_1^+-A_1^-$  ion pair ( $1/k'_{-2}$ ) than to its effect on the rate of formation of this state ( $k'_2$ ) at pump pulse separation times of hundreds of picoseconds. The time constant for recombination of the  $A_2^--D_2^+$  state to the ground state in the presence of the  $D_1^+-A_1^-$  ion pair ( $1/k'_{-2}$ ) is  $140 \pm 30$  ps, whereas with the  $D_1-A_1$  pair in its neutral state the time constant for recombination of the  $A_2^--D_2^+$  state ( $1/k_{-2}$ ) is 1.3 ns. The fits are only weakly dependent on variations in  $k'_2$ , and we were unable to determine this parameter beyond the restriction

that  $k'_2 \leq 2 \text{ ns}^{-1}$ . Thus, the data in Fig. 2 suggest that the slow formation and decay of the  $A_2^--D_2^+$  state is disrupted during the short lifetime of the  $D_1^+-A_1^-$  state because the electric field generated by the  $D_1^+-A_1^-$  state makes recombination of the  $A_2^--D_2^+$  state to the ground state (140 ps) considerably faster than formation of the  $A_2^--D_2^+$  state ( $>500$  ps).

The mechanism of this electric field-induced 10-fold increase in the  $A_2^--D_2^+$  recombination rate can be analyzed within

the context of electron transfer theory (27, 28) by considering the possible effects of the electric field produced by  $D_1^+-A_1^-$  on the free energy, the total nuclear reorganization energy, and the electronic coupling matrix element,  $V$ , for the charge recombination reaction. The free energy for charge separation within  $A_2^--D_2^+$  alone,  $\Delta G_{CS}$ , cannot be more negative than  $-0.3$  eV, as estimated from the lowest excited singlet-state energy of  $D_2$ , the electrochemical potentials for one-electron oxidation and re-

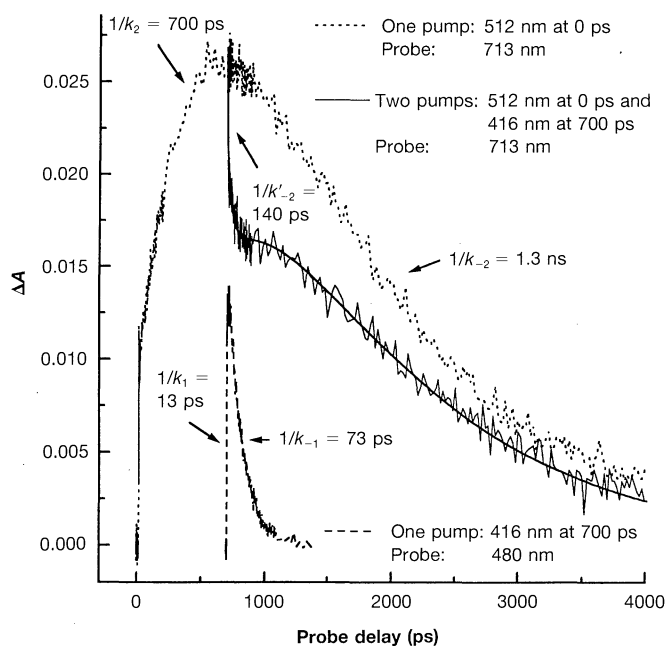


**Fig. 2.** Transient absorption kinetics ( $\Delta A$ ) of  $D_1-A_1-A_2-D_2$  in 1,4-dioxane excited with one pump pulse at 416 nm, one pump pulse at 512 nm, and two sequential pump pulses at 416 and 512 nm at the times indicated. The given rate constants correspond to those labeled in Fig. 3.

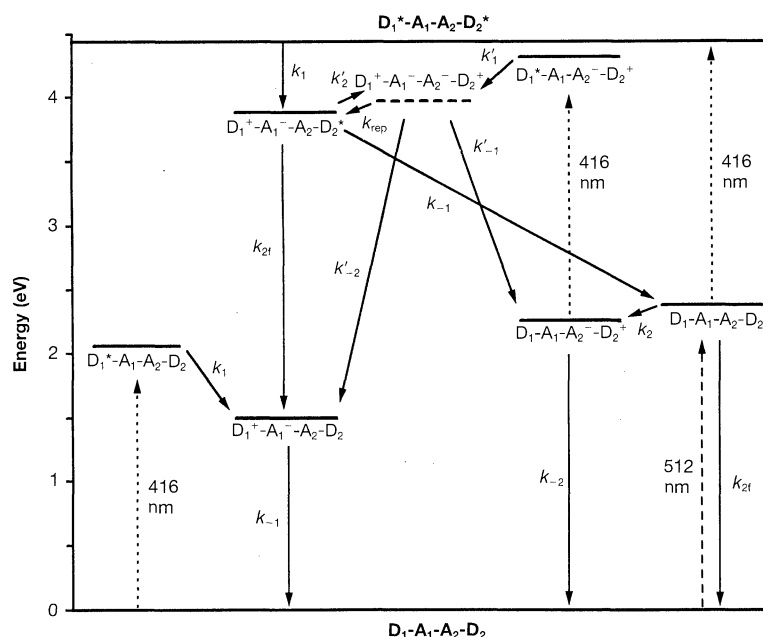


**Fig. 3.** Scheme used to model the kinetics of electron transfer in  $D_1-A_1-A_2-D_2$  in 1,4-dioxane (24). Solid arrows depict ion pair formation, ion pair decay, and excited-state decay processes and are labeled with their respective rate constants  $k$ . Photoexcitation processes are depicted with dashed arrows.

duction of  $D_2$  and  $A_2$ , respectively, and the Coulomb interaction energy between the two ions (24). The corresponding free energy for charge recombination,  $\Delta G_{CR}$ , cannot be more positive than  $-2.1$  eV (24). Rapid, laser-induced formation of  $D_1^+-A_1^-$  adjacent to  $A_2^-D_2^+$  changes the total Coulombic interaction energy within the ensemble of four ions. As a result of the Coulomb interaction of the adjacent ion pairs, the energy of the  $D_1^+-A_1^-A_2^-D_2^+$  state in 1,4-dioxane is  $\sim 0.21$  eV greater than the sum of the energies of the  $D_1^+-A_1^-A_2^-D_2$  and  $D_1^+-A_1^-A_2^-D_2^+$  states. A pairwise breakdown of the interaction energies of the ions (Table 1) (29) shows that the  $A_1^-A_2^-$  and  $D_1^+-D_2^+$  ion pairs contribute repulsion energies of 0.65 eV and 0.22 eV, respectively, but this is largely compensated by the attractive forces within the  $D_1^+-A_2^-$  and  $A_1^-D_2^+$  pairs. If the energy of the  $D_1^+-A_1^-A_2^-D_2^+$  state is above that of  $D_1^+-A_1^-A_2^-D_2^*$ , partial repopulation of the  $D_1^+-A_1^-A_2^-D_2^*$  state may occur, resulting in an increase in stimulated emission from  $D_2^*$ . However, there was no significant difference ( $<5\%$ ) in the observed stimulated emission intensities from  $D_2^*$  monitored at 553 nm between the one-pump and two-pump experiments. In addition, the data in Fig. 2 could not be fit accurately with the inclusion of a predominant rate constant for repopulation of  $D_1^+-A_1^-A_2^-D_2^*$  in the kinetic model. These results suggest that recombination of  $A_2^-D_2^+$  to its ground state within  $D_1^+-A_1^-A_2^-D_2^+$  is faster than excited-state repopulation leading to  $D_1^+-A_1^-A_2^-D_2^*$ .

The free energy of the charge recombination reaction within  $A_2^-D_2^+$  is  $\leq -2.1$  eV, and therefore this reaction is most likely well into the Marcus inverted region (27). Thus, destabilizing  $A_2^-D_2^+$  by 0.21 eV makes  $\Delta G_{CR}$  more negative and should result in a decrease in the charge recombination rate, not the increase that is observed (27, 28). In addition, generating  $D_1^+-A_1^-$  at a fixed distance and orientation relative to  $A_2^-D_2^+$  within a low-polarity solvent should have a negligible effect on the total reorganization energy for

charge recombination within  $A_2^-D_2^+$  (30). On the other hand, the electronic coupling matrix element between  $A_2^-$  and  $D_2^+$  may be increased by electronic repulsion between the singly occupied molecular orbitals in  $A_1^-$  and  $A_2^-$ . This increase in  $V$  should result in an even larger increase in the rate constant for charge recombination,  $k_{CR}$ , because  $k_{CR} \propto V^2$  (27, 28). Analogous arguments can be made focusing on the rates of charge separation and recombination within  $D_1^+-A_1^-$ , which are influenced by the electrostatic effects of the ions within  $A_2^-D_2^+$ .

This analysis suggests that the rapid creation of the  $D_1^+-A_1^-$  dipole modifies the electronic environment in the vicinity of  $A_2^-D_2^+$ . These environmental changes can be imposed in a rapid and controlled fashion by means of ultrafast laser pulses. Even larger field effects might be observed if the two donor-acceptor pairs are positioned side by side. Our results suggest that this type of molecular architecture has many of the characteristics required of a prototype molecular switch, the most notable of which is the rapid control of state switching by femtosecond optical pulses.

## REFERENCES AND NOTES

- J. J. Hopfield, J. N. Onuchic, D. N. Beratan, *Science* **241**, 817 (1988).
- J.-M. Lehn, *Angew. Chem. Int. Ed. Engl.* **27**, 89 (1988).
- M. Mehring, in *Electronic Properties of Conjugated Polymers III*, vol. 91 of *Springer Series in Solid-State Sciences*, M. Mehring and S. Roth, Eds. (Springer-Verlag, Berlin, 1989), pp. 242-249.
- M. P. O'Neil et al., *Science* **257**, 63 (1992).
- M. R. Wasielewski, *Chem. Rev.* **92**, 435 (1992).
- R. W. Wagner, J. S. Lindsey, J. Seth, V. Palaniappan, D. F. Bocian, *J. Am. Chem. Soc.* **118**, 3996 (1996).
- A. Aviram and M. A. Ratner, *Chem. Phys. Lett.* **29**, 277 (1974).
- A. Aviram, *J. Am. Chem. Soc.* **110**, 5687 (1988).
- A. Broo, *Chem. Phys.* **169**, 135 (1993).
- J. M. Tour, R. Wu, J. S. Schumm, *J. Am. Chem. Soc.* **113**, 7064 (1991).
- F. Garnier, G. Horowitz, X. Peng, D. Fichou, *Adv. Mater.* **2**, 592 (1990).
- J. R. Sambles and A. S. Martin, *Phys. Scr.* **149**, 718 (1993).
- H. Kuhn, *Pure Appl. Chem.* **53**, 2105 (1985).
- E. G. Wilson, *Jpn. J. Appl. Phys.* **34**, 3775 (1995).
- E. Galoppini and M. A. Fox, *J. Am. Chem. Soc.* **118**, 2299 (1996).
- D. Gosztola, H. Yamada, M. R. Wasielewski, *ibid.* **117**, 2041 (1995).
- M. P. Debreczeny, W. A. Svec, M. R. Wasielewski, *New J. Chem.* **20**, 735 (1996).
- The compounds shown in Fig. 1 were characterized by proton nuclear magnetic resonance (NMR), mass spectral analysis, and ultraviolet (UV)-visible spectroscopy. Proton NMR spectra were obtained on a 300-MHz Bruker AM-300 spectrometer. Mass spectra were obtained with a Kratos MALDI spectrometer. UV-visible spectra were obtained with a Shimadzu UV-160 spectrometer. Merck silica gel 60 was used for column chromatography. All solvents were reagent grade. 1,4-Dioxane was refluxed over  $LiAlH_4$ , distilled, and stored under nitrogen.
- Transient absorption data were obtained with a regeneratively amplified Ti:sapphire laser (16). This laser produced pulses of 416 nm, 130 fs, and 100  $\mu$ J at a 1.3-kHz repetition rate. For the experiments

with pump pulses at both 416 and 512 nm, 90% of the energy of the 416-nm pulses was used to pump a two-stage optical parametric amplifier that furnished 150-fs transform-limited pulses at 512 nm with energies up to 6  $\mu$ J per pulse [S. R. Greenfield and M. R. Wasielewski, *Opt. Lett.* **20**, 1394 (1995)]. A 150-fs white-light probe beam, the color of which was selected by a monochromator after the sample, was used for probing. The probe spot size was kept smaller than either of the two pump beams, and all three beams overlapped inside the stirred sample (path length, 1 mm). In the kinetic measurements, the arrival times of the two pumps were fixed relative to each other and the probe arrival time was varied. The 512-nm pump pulses were chopped synchronously at half of the 1.3-kHz repetition rate of the laser so that every other pulse was blocked; the 416-nm pump pulses were not chopped. Therefore, the  $D_1^+-A_1^-$  charge-separated state was generated with every 416-nm pulse, but the  $A_2^-D_2^+$  charge-separated state was generated with every other 512-nm pulse. When this arrangement and a 713-nm probe pulse are used to observe the population of  $A_2^-$ , the transient absorption signal is proportional to the population of the  $A_2^-D_2^+$  state.

- A. Viehbeck, M. J. Goldberg, C. A. Kovac, *J. Electrochem. Soc.* **137**, 1460 (1990).
- A. Osuka et al., *J. Am. Chem. Soc.* **115**, 9439 (1993).
- M. Gouterman, in *The Porphyrins*, D. Dolphin, Ed. (Academic Press, New York, 1978), vol. 3, pp. 1-165.
- By optimizing the sample concentration and pump intensity, we could excite a large population of the  $D_1$  chromophores in the probed sample volume, as demonstrated by a leveling off of the transient absorption signal due to the formation of  $A_1^-$  within  $D_1^+-A_1^-$  with increasing pump intensity. In contrast, the  $D_2$  chromophore, which has a lower absorption cross section and was typically excited with lower pump intensities, was in the regime where the magnitude of the observed transient absorption signal was linear with the pump intensity.
- The excited-state energies ( $E_s$ ) of donors  $D_1$  and  $D_2$ , estimated from the mean of their respective room-temperature absorption and fluorescence maxima in 1,4-dioxane, are 2.06 and 2.38 eV, respectively. The free energies of formation of the ion pairs ( $\Delta G_{D^+A^-}$ ) relative to their neutral ground states in polar solvents were calculated according to

$$\Delta G_{D^+A^-} = E_{OX} - E_{RED} - \frac{e_0^2}{\epsilon_S r_{DA}}$$

where  $E_{OX}$  and  $E_{RED}$  are the one-electron oxidation and reduction potentials of the donor and acceptor, respectively, in the high-polarity solvent butyronitrile;  $e_0$  is the electronic charge;  $\epsilon_S$  is the static dielectric constant of butyronitrile (25); and  $r_{DA}$  is the distance between the ions within each pair (Table 1).  $D_1$  and  $D_2$  oxidize at 0.62 and 1.31 V versus SCE (saturated calomel electrode), respectively.  $A_1$  and  $A_2$  reduce at  $-0.46$  and  $-0.65$  V versus SCE, respectively.  $\Delta G_{D^+A^-}$  is the lowest estimated energy for the ion pair states because these states should be destabilized somewhat within the lower polarity solvent 1,4-dioxane. The exact magnitude of this destabilization is difficult to assess because 1,4-dioxane has higher order multipole moments in its charge distribution [J. Warman et al., *Chem. Phys.* **170**, 359 (1993)].

- Control experiments performed on molecules consisting of only  $D_1-A_1$  or  $A_2-D_2$  have demonstrated that the two-pump effect is dependent on the presence of both donor-acceptor pairs within the same molecule. For  $D_1-A_1-A_2-D_2$ , if the 416-nm pump pulse is set to arrive before or at the same time as the 512-nm pump pulse, the 416-nm pump pulse does not cause a change in the transient absorption signal that monitors the population of  $A_2^-$ . The difference between the one-pump and two-pump transient absorption signals is largest when the 512-nm pump pulse is set to arrive hundreds of picoseconds earlier than the 416-nm pump pulse, and this difference is greatly reduced when the two pump pulses arrive simultaneously; hence, exciton annihilation is not re-

**Table 1.** Energetics of the Coulomb interaction between the adjacent ion pairs in  $D_1^+-A_1^-A_2^-D_2^+$  in 1,4-dioxane (25).

Ion pair	Distance (Å)	Energy shift (eV)
$A_1^-A_2^-$	12.2	+0.65
$A_1^-D_2^+$	23.4	-0.34
$D_1^+-A_2^-$	25.1	-0.32
$D_1^+-D_2^+$	36.3	+0.22
Total		+0.21

sponsible for the effect. Excitation energy transfer between the  $D_1$  and  $D_2$  chromophores (leading to exciton annihilation if the two are simultaneously excited) can also be ruled out by observation of the evolution of the transient absorption spectra when using only a single pump. Selective excitation of each donor in  $D_1$ - $A_1$ - $A_2$ - $D_2$  ( $D_1$  at 416 nm,  $D_2$  at 512 nm) leads to the selective appearance of the anion spectrum of the acceptor adjacent to the donor that is excited. The anion absorption spectra of the two acceptors are readily distinguishable due to their sharp and distinctive features. This observation also allows us to rule out the possibility of electron transfer from  $D_1$ - $A_1$ - $A_2$ - $D_2^+$  to  $D_1$ - $A_1$ - $A_2$ - $D_2^+$ . This process, although energetically favorable, is presumably too slow to compete with recombination of  $A_2^-$ - $D_2^+$  to the ground state.

26. W. Liptay, in *Excited States*, E. C. Lim, Ed. (Academic Press, New York, 1974), pp. 129-229.
27. R. A. Marcus, *J. Chem. Phys.* **43**, 679 (1965).
28. J. Jortner, *ibid.* **64**, 4860 (1976).
29. The Coulomb energies were calculated by the point

monopole approximation. The centers of charge in the charge distributions on  $D_1$ ,  $A_1$ ,  $A_2$ , and  $D_2$  in going from the neutral to the charge-separated states were computed by the AM1 algorithm using an MM2 geometry-optimized model of  $D_1$ - $A_1$ - $A_2$ - $D_2$ . The molecular mechanics calculations were performed using a modified MM2 model within Hyperchem (Hypercube, Waterloo, Ontario). Coulomb energies in 1,4-dioxane were related to in vacuo energies by means of the spherical cavity approximation [W. Liptay, in *Modern Quantum Chemistry*, O. Sinanoglu, Ed. (Academic Press, New York, 1965), vol. 3, pp. 45-66; C. J. F. Böttcher, *Theory of Electric Polarization* (Elsevier Scientific, Amsterdam, ed. 2, 1973), vol. 1].

30. A. Farazdel, M. Dupuis, E. Clementi, A. Aviram, *J. Am. Chem. Soc.* **112**, 4206 (1990).
31. Supported by the Office of Computational and Technological Programs, Division of Advanced Energy Projects, U.S. Department of Energy, under contract W-31-109-ENG-38.

27 June 1996; accepted 27 August 1996

## Interlayer Tunneling Models of Cuprate Superconductivity: Implications of a Recent Experiment

A. J. Leggett

It is shown that, given a few generic assumptions, any theory of high-temperature superconductivity that attributes a substantial fraction of the condensation energy to the saving of  $c$ -axis kinetic energy must predict an inequality relating the  $c$ -axis penetration depth  $\lambda_{\perp}(0)$  to the zero-temperature superconducting-normal energy difference and the fluctuations of the  $c$ -axis kinetic energy around its mean value. Application of this formula to  $Tl_2Ba_2CuO_6$  implies that if  $\lambda_{\perp}(0)$  is greater than 10 micrometers, as suggested by a recent experiment, these fluctuations must have an unusual form.

Of the many and varied approaches to the high-temperature superconductivity (HTS) problem currently available, none is more novel or intriguing than the interlayer tunneling (ILT) model of Anderson and co-workers (1-4). This model rests on two major postulates: (i) The normal state of the electrons within a single  $CuO_2$  plane is different in nature from the traditional Landau Fermi liquid, and (ii) as a result, single-particle tunneling between the  $CuO_2$  planes is strongly inhibited in the normal phase; however, in the superconducting phase, tunneling of pairs is possible and results in a strong decrease of the  $c$ -axis kinetic energy  $T_{\perp}$ . Thus, depending on the particular version of the model considered, either all or, at least in the cuprates with higher transition temperatures  $T_c$ , a large fraction of the condensation energy  $E_{cond}$  (the difference between the superconducting ground-state energy and the "best" normal-state energy) comes from the decrease of  $\langle T_{\perp} \rangle$  (brackets denote expectation value) in the superconducting state. In this report,

I shall take this last statement as the definition of the ILT model, irrespective of the way in which point (i) is implemented.

The ILT model has a number of attractive features. It explains in a natural way why all materials known to date with  $T_c > 35$  K have well-separated planes in which the electronic behavior appears to be two-dimensional (2D) in the first approximation, and why despite the apparent similarity of the in-plane behavior, the values of  $T_c$  for the various cuprates vary by a factor of more than 20. The model obviates the need for an anomalously strong in-plane attraction mechanism, and it can be argued (2) to be consistent with a variety of apparently puzzling experimental properties of the cuprates, in particular (4) with the normal- and superconducting-state finite-frequency  $c$ -axis conductivity. It is therefore important to explore the generic consequences of the ILT model and to examine their compatibility with existing experimental data.

For this purpose, I confine myself to those ("single-plane") cuprates in which all pairs of neighboring  $CuO_2$  planes are equivalent. In this case, various particular

implementations of the ILT model [see especially (3)] lead to an expression for the  $T = 0$  interplane coupling energy  $E_{int}$  (which in these versions is the difference between the normal- and superconducting-state values of  $\langle T_{\perp} \rangle$ ) that is a special case of the more general Lawrence-Doniach (LD) expression (given for a particular pair of planes  $i, i + 1$ )

$$E_{int}^{LD} = K - J \cos \Delta \phi_i^{(pair)} \quad (1)$$

where  $\Delta \phi_i^{(pair)}$  is the difference in the phase of the superconducting order parameter between the two planes in question, and  $K$  and  $J$  are material-dependent constants. In non-ILT theories, which simply regard the interplane tunneling process as described by the original Josephson model (5) for a tunnel oxide barrier and naïvely apply the Ambegaokar-Baratoff expressions (6), one finds that  $K \approx J$ , and hence in the superconducting ground state [ $\Delta \phi_i^{(pair)} = 0$ ], no appreciable energy is saved by tunneling. However, in the current form of the ILT model (3, 4),  $K$  is postulated to be zero, or at any rate,  $K \ll J$ . If this is so, one obtains a relation between the saving of  $c$ -axis kinetic energy in the superconducting ground state,  $\Delta T_{\perp}^{ns}$ , and the  $T = 0$   $c$ -axis superfluid density  $\rho_{s\perp}$ : for  $K = 0$

$$\Delta T_{\perp}^{ns} = \left( \frac{\hbar}{2md} \right)^2 \rho_{s\perp} \quad (2)$$

where  $m$  is the electron mass and  $d$  is the interplanar spacing. In the ILT model,  $\Delta T_{\perp}^{ns}$  supplies a substantial fraction  $\eta$  of the superconducting condensation energy, which, as pointed out by Anderson (4), leads to a definite prediction for the  $T = 0$   $c$ -axis penetration depth  $\lambda_{\perp}(0)$ . For our purposes, it is convenient to write this prediction in the form

$$\lambda_{\perp} = \frac{1}{2} \eta^{-1/2} \lambda_{ILT}, \quad \lambda_{ILT} = \left( \frac{mc^2 a_0 A}{E_{cond} 4\pi d} \right)^{1/2} \quad (3)$$

where  $c$  is the speed of light,  $E_{cond}$  is the superconducting condensation energy per formula unit,  $a_0$  is the Bohr radius, and  $A$  is the area per formula unit. (The precise definition of  $\lambda_{ILT}$  is chosen with a view to giving Eq. 7 below a simple form.) A case of particular interest is  $Tl_2Ba_2CuO_6$  (Tl-2201), where  $\lambda_{ILT} \sim 1.8 \mu m$ . Recently, van der Marel *et al.* (7) concluded, on the basis of the absence of a  $c$ -axis plasmon peak in their optical reflectivity measurements, that  $\lambda_{\perp}(0)$  must be  $> 10 \mu m$ . From Eq. 3, this implies that  $\eta < 0.01$  in this material; this conclusion holds for any positive value of  $K$  in Eq. 1.

A value of  $\lambda_{\perp}(0) > 10 \mu m$  in Tl-2201, if confirmed, would thus seem to refute definitively any version of the ILT model, such

Department of Physics, University of Illinois at Urbana-Champaign, Urbana, IL 61801, USA.